How Stretchable Can We Make Thin Metal Films?

Candice Tsay[1], Stephanie P. Lacour[1], Sigurd Wagner[1], Teng Li[2], Zhigang Suo[2]
[1]Department of Electrical Engineering, Princeton University, Princeton, NJ, USA
[2]Division of Engineering and Applied Sciences, Harvard University, Cambridge, MA, USA

ABSTRACT

Thin metal films deposited on elastomeric substrates can remain electrically conducting at tensile strains up to ~100%. We recently used finite-element simulation to explore the rupture process of a metal film on an elastomer. The simulation predicted the highest stretchability on stiff elastomeric substrates [1]. We now report experiments designed to verify this prediction. A ~15-μm thick silicone elastomer layer with Young's modulus E ~ 160 MPa is deposited on a 1mm thick membrane of polydimethylsiloxane (PDMS), a silicone elastomer with E ~ 3 MPa. Metal stripes consisting of 25-nm thick gold (Au) film sandwiched between two 5-nm thick chromium (Cr) adhesion layers are fabricated either on top of the stiff layer spun onto the soft membrane substrate, or are encapsulated at the interface between the two elastomers. Encapsulated gold films remain electrically conducting beyond 40% strain. But conductors deposited on top of stiff elastomer lose conduction at strains of 3-8%. These results suggest that, in addition to the stiffness of the elastomeric substrate, the initial microstructure of the metal film plays a role in determining its stretchability.

INTRODUCTION

Conformable or skin-like electronics must withstand repeated and large deformations. For example, a stretchable sensor array wrapped around the elbow-joint of a prosthetic arm may experience tensile strains of 10% or more. However, thin film electronic materials fracture at lower strains than this. Free-standing gold films, for example, rupture at 1-2% strain [2].

We have demonstrated experimentally that a thin gold film bonded to an elastomeric substrate with Young's modulus E ~ 3 MPa can stretch and remain conducting to 100% strain [3, 4]. This is a step toward fabricating elastic electronic circuits on elastomeric substrates using arrays of rigid device islands connected by stretchable metallization [5]. We used finite-element simulations to model the rupture process for these stretchable conductors. The results show that, while freestanding metal films rupture by deformation localization, an elastomeric substrate suppresses the localization and allows the metal film to elongate without immediate rupture [1, 6]. Furthermore, the simulation predicts greater stretchability for metal films on stiffer elastomeric substrates. This paper describes experiments designed to test the simulation prediction and also presents our observations on the effect of an encapsulating silicone layer on the conductor's stretchability.

Four types of samples are prepared, summarized in Figure 1a. Type A, in which the gold conductor is fabricated on top of the compliant silicone (E ~ 3 MPa) substrate, is the configuration tested many times before [3, 4], and is used here as a basis for comparison. For type B, we introduce a moderately stiff silicone material (E ~ 160 MPa) as the substrate. The ~15-μm thick stiff silicone layer is spun onto the 1-mm thick compliant silicone substrate for easier handling. Given the large compliance of the 1-mm substrate, the metal film behaves mechanically as if it were attached to the stiff elastomer alone. For the other two configuration

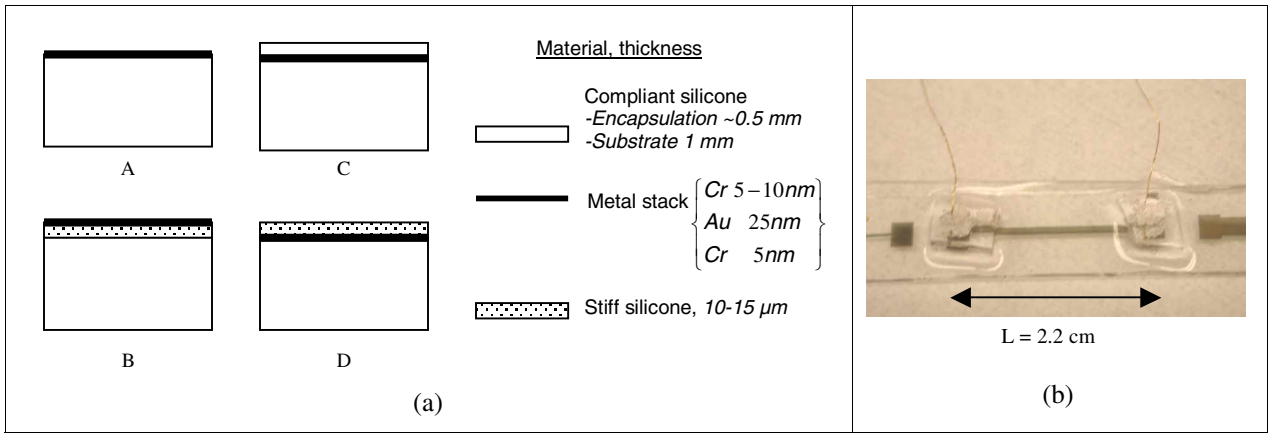

Figure 1. (a) Cross-section views. Type A: compliant silicone (E ~ 3 MPa) as substrate; type B: stiff silicone (E ~ 160 MPa) bottom layer; type C: compliant silicone encapsulation; type D: stiff silicone encapsulation. (b) Top view photograph of a type C conductor 600-μm wide with embedded gold wires and compliant PDMS on top.

types, the gold conductor is sandwiched between the compliant silicone substrate and an encapsulating silicone film. For type C, the compliant silicone is used as the top encapsulating material. Figure 1b shows a conductor encapsulated by the clear, compliant silicone and lead wires to the contact pads. For type D, the stiff silicone is used as the top encapsulating material.

EXPERIMENTAL DETAILS

Sample preparation

The compliant silicone substrate material (Sylgard 184®, Dow Corning) is cast in a plastic Petri dish and oven-cured at 60ºC to a 1-mm thick PDMS membrane. Electron-beam evaporation is used to deposit the metal through a polyimide shadowmask [3]. The metal film consists of a 25-nm thick Au layer between two 5-nm thick Cr layers. The thin Cr layers are needed for the adhesion of Au to the adjoining PDMS. After the deposition, the shadowmask is peeled away, resulting in conductors that are 2-cm long and 600-μm wide.

The stiff silicone (WL-5150 photo-patternable silicone, Dow Corning) is spin-coated either on top of the compliant PDMS membrane (for type B) or on top of the metallic conductor (for type D), then oven-cured at 80ºC for 10 hours. The film is typically 10 to 15-μm thick. For the conductors with the stiff silicone underneath, the silicone is spun on and cured before metal deposition.

When the stiff silicone is spun directly onto the conductors, the substrate, i.e. the compliant PDMS membrane, is mounted on a 0.5-mm thick aluminum sheet prior to metal deposition. The aluminum backing provides stability and rigidity during the subsequent spinning and baking steps. After metal deposition, the stiff silicone is spun on top of the conductors to 10 to 15-μm thickness and is then patterned to open contact holes to the conductor pads. The patterning process is similar to a photoresist process: a UV exposure, a 150ºC baking step for polymerization, and a solvent development [9]. After the silicone film is cured, the aluminum backing is removed in an HCl etching solution.

The symmetrically encapsulated conductors (type C) are topped with Sylgard 184 PDMS after electrical connections are established. To ensure contact, 100-μm diameter gold wires are first attached to the conductor pads with uncured epoxy-based conductive paste. The PDMS is

then hand-deposited on the areas surrounding the pads. After a 60°C oven-cure, the gold wires are effectively embedded in the PDMS (Fig. 1b).

Sample characterization

For electromechanical measurements, compliant electrical contacts are made to the conductors using the same method as described above for the symmetric encapsulated conductors. Electrical resistance is recorded with a Keithley 4140 source-meter.

The uni-axial stretching is done with an automated stretching device [3]. Data acquisition and control of the stepper motor is done through a Labview program. In all experiments, the strain is increased in steps of 0.1% every 12 seconds.

For Scanning Electron Microscopy observation, the samples are coated with a 5-nm thick iridium layer.

RESULTS

Type A and type B. No encapsulating layer.

We compare the stretchability of type A and type B samples. The electrical resistance is measured as the sample is stretched with increasing applied tensile strain and plotted in Figures 2a and 2b. Surprisingly, the conductors on the stiff silicone do not retain electrical conduction at as high strains as the conductors on the compliant silicone. The electrical resistance of the conductor on complaint silicone (type A) increases steadily with the applied strain. At 50% strain, its resistance has increased by over 1200%, but the sample does not fail electrically and no macroscopic cracks appear in the film. Instead, as shown in Fig. 2c, the metal usually buckles, by Poisson compression, in the direction perpendicular to the applied strain [7]. After relaxation

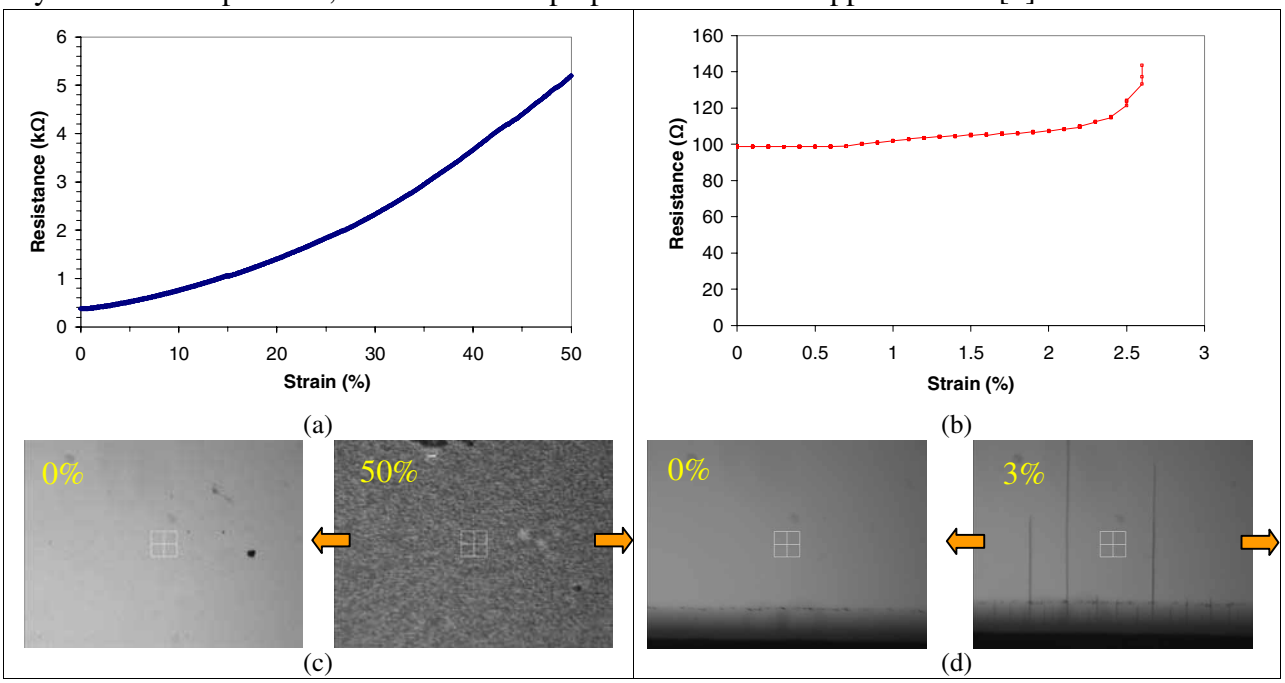

Figure 2. Electrical resistance as a function of applied tensile strain for (a) a gold conductor on compliant silicone; (b) a gold conductor on stiff silicone. 320-µm x 240-µm optical micrographs of (c) top surface of metal of sample in (a) during stretch at 0% and 50% strain; and (d) top surface of metal of sample in (b) during stretch at 0% and 3% strain. Arrows indicate stretching direction.

back to 0% strain, the resistance value recovers to a value slightly higher than the pre-stretch initial resistance value.

In contrast, electrical failure occurs at 3% strain for the conductor on the stiff silicone. Multiple small transversal cracks form at the edges of the conductor and gradually traverse across the width of the line, as seen in Figure 2d. Loss of conduction corresponds to the moment in which cracks from opposite edges meet to form a line of discontinuity across the width of the metal. After relaxation to 0% strain, electrical conduction returns, but parallel cracks are visible in the metal layer. All 600-µm wide samples of this type display this behavior, and none retain conduction above 8% strain.

In addition, although the two sample types are prepared in the same metallization batch, the samples on stiff silicone have four times lower initial resistance than the samples on compliant silicone. This disparity may be explained by considering surface roughness of the silicone materials. The surface roughness of gold on the compliant silicone is twice that of gold on the stiff silicone [8]. The difference is clear in the SEM micrographs shown in Figure 3.

Type C and type D. With encapsulating layer.

All encapsulated conductors are highly stretchable, regardless of the coating layers' stiffness. Figure 4a shows the normalized resistance ($R/R_{initial}$) plotted against tensile strain for the two encapsulated configurations as well as the non-encapsulated conductor on compliant silicone. Both the resistance values and the metal morphology follow closely those of a non-covered conductor. The samples can be stretched beyond 30% strain, but this particular compliant silicone encapsulated sample slipped from the stretching apparatus during the test. Encapsulated samples and non-encapsulated samples fabricated in the same metallization batch

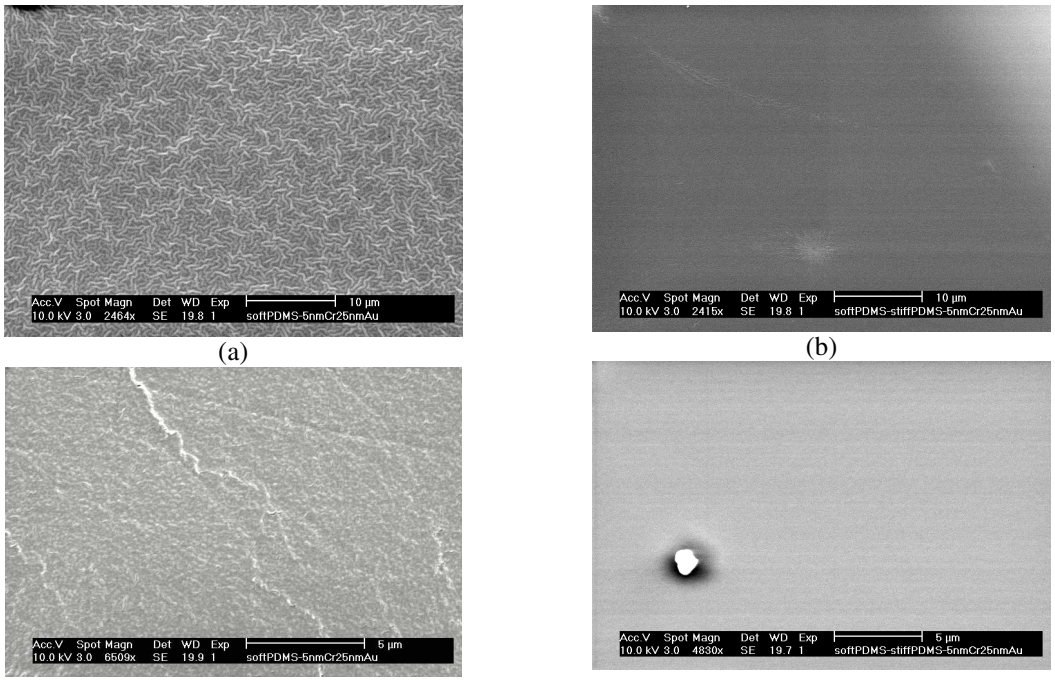

Figure 3. SEM micrographs of (a, top) a bare compliant silicone surface; (a, bottom) 5-nm Cr and 25-nm Au on compliant silicone; (b, top) a bare stiff silicone surface; (b, bottom) 5 nm-Cr and 25-nm Au on stiff silicone. Samples have been coated with 5-nm iridium.

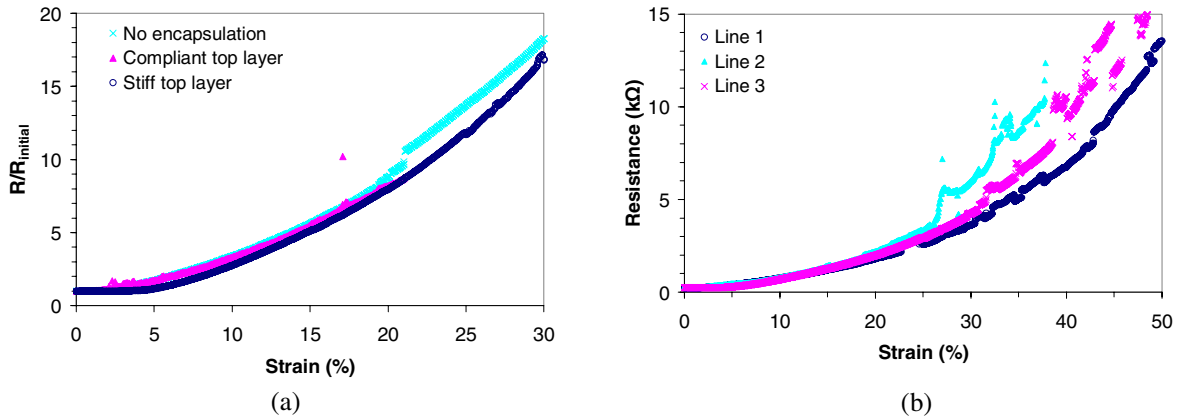

(a) (b)

Figure 4. Electrical resistance measured with increasing applied strain. (a) Normalized resistance of conductors with stiff silicone encapsulation, compliant PDMS encapsulation, and no encapsulation; (b) Three conductors with stiff encapsulation.

all fail electrically near the same critical strain. Figure 4b shows the electrical resistance values measured with increasing strain for three stiff silicone-covered conductors of the same batch.

Two different conductor widths, 350-µm and 600-µm, are also tested for each configuration. Wider conductors have lower initial resistance in every case and generally retain conduction at higher strains. The effect is more pronounced for the conductors on stiff silicone.

CONCLUSIONS

The present experiments show that using the stiff elastomer as the substrate material does not increase stretchability of the metal film, although the simulation predicted highest stretchability on stiff elastomeric substrates. This discrepancy in metal film stretchability is explained as follows. Rupture of thin metal film results from localized plastic deformation [2] such as necking or shear-off. A polymer substrate delocalizes the deformation in a metal film under tension, thus carrying the film to large strain before rupture [6]. In the finite-element simulation, good adhesion between the metal film and the elastomer substrate is assumed, thus excluding delamination along the film/substrate interface. Under such an assumption, a stiffer elastomer substrate more effectively delocalizes the deformation in the metal film, thus leading to better stretchability of the film. In practice, the metal/elastomer interface is never perfect. When such a structure is stretched, debonding may occur, so that the metal film becomes freestanding and ruptures at a small strain. The adhesion between the metal film and the elastomer substrate is critical to the stretchability of the metal film [10]. The formation of multiple transverse cracks in the metal conductor (as in Fig. 2d) has also been observed in metal films on polymer substrates by other researchers [10]-[12]. This rupture behavior of the metal conductor on a stiff elastomer suggests weak adhesion between the film and the substrate, which leads to poor stretchability of the metal conductor.

Another type of rupture behavior is observed in gold films deposited directly on the compliant silicone substrate. While we have previously observed two types of gold film on compliant silicone – buckled and smooth, or flat and microstructured [7] - the samples tested in the current experiment appear to be the latter. These gold films display a complex

microstructure that results from the surface roughness of the underlying substrate. This microstructure is not reflected in the finite-element simulation model. Experimentally, these samples retain electrical conduction at very high strains without rupturing. This suggests that the gold film's initial microstructure plays an important role in determining its stretchability.

This study also finds that depositing another elastomer layer on top of a stretchable conductor does not significantly change the electrical behavior of the metal film during stretching. Cycling experiments can be done to see if the encapsulation improves the fatigue life of the conductors.

ACKNOWLEDGMENT

This research was supported by DARPA-funded AFRL-managed Macroelectronics Program Contract FA8650-04-C-7101, and by the New Jersey Commission on Science and Technology.

REFERENCES

1. T. Li, Z. Huang, Z. Suo, S. P. Lacour, S. Wagner, Appl. Phys. Lett. **85**, 3435 (2004).
2. D.W. Pashley, Proc. Roy. Soc. Lond. A **255**, 218 (1960).
3. S.P. Lacour, S. Wagner, Z. Huang, Z. Suo, Appl. Phys. Lett. **82**, 2404 (2003).
4. S.P. Lacour, J. Jones, Z. Suo, S. Wagner, IEEE Elec. Dev. Lett. **25**, 179 (2004).
5. S.P. Lacour, C. Tsay, S. Wagner, IEEE Elec. Dev. Lett. **25**, 792 (2004).
6. T. Li, Z. Y. Huang, Z. C. Xi, S. P. Lacour, S. Wagner, and Z. Suo, Mechanics of Materials **37**, 261 (2005).
7. C. Chambers, S.P. Lacour, S. Wagner, Z. Suo, Z. Huang, Mat. Res. Soc. Symp. Proc. **769** Apr. 2003, pp. H10.3.1-6.
8. W. Zhang, J.P. Labukas, S. Tatic-Lucic, L. Larson, T. Bannuru, G.S. Ferguson, Technical Digest Eurosensors XVIII (Rome, 2004), 552.
9. H. Meynen, M. Vanden Bulcke, M. Gonzalez, B. Harkness, G.Gardner, J. Sudbury-Holtschlag, B. Vandevelde, C. Winters, E. Beyne, Microelec. Eng. **76**, 212 (2004).
10. Y. Xiang, T. Li, Z. Suo, J.J. Vlassak, to be pubished.
11. S. L. Chiu, J. Leu and P. S. Ho, J. Appl. Phys., **76**, 5136 (1994).
12. B. E. Alaca, M. T. A. Saif and H. Sehitoglu, Acta Mater., **50**, 1197 (2002).